SURGICAL MICROPOROUS CAPACITIVE PRESSURE SENSORS: A GOOD USE FOR TABLE SUGAR

by

Diana T. Vera

A THESIS SUBMITTED TO THE GRADUATE DIVISION OF THE UNIVERSITY OF HAWAI ʻI AT MĀNOA IN PARTIAL FULFILLMENT OF THE REQUIREMENTS FOR THE DEGREE OF

MASTER OF SCIENCE

IN

ELECTRICAL ENGINEERING

Thesis Committee:

Aaron T. Ohta, Chairperson

David Garmire

Victor Lubecke

May 2017

Acknowledgments

I want to thank my advisor Aaron T. Ohta for the opportunity to join his amazing team and for all his help in ensuring my success as a Masters student. Through his guidance, I have learned how to make various sensors through trial and error. The experience I gained from this project has helped harvest a greater sense of perseverance in myself.

I want to give a special thanks to Maurice Garcia, whose enthusiasm and advice helped guide me through completion of this project and my degree.

Deep thanks to my lab mates for their assistance in this project. Although I am miles away from home we made each other feel like family.

Thanks to David Garmire and Victor Lubecke for accepting to be a part of my thesis committee.

I also want to thank my family and friends for their love and support.

Abstract

By

Diana T. Vera

Master of Science in Electrical Engineering

University of Hawai‘i, Mānoa

Aaron T. Ohta, Chair

Pressure analyses play a crucial role in the automotive and medical industries. Pressure sensors in the medical industry are used for minimally invasive surgeries and the self-monitoring of vital signals without the aid of a healthcare professional. The fabrication of smaller pressure sensors can lead to increased comfort during surgery and an improved surgical experience for doctors, and more importantly, patients. This paper introduces five microporous capacitive pressure sensors made from microporous polydimethylsiloxane dielectric layers and copper electrodes. To achieve higher sensitivity, granulated sucrose was added to the pre-polymer base and curing agent of varying weight ratios. The most sensitive device was tested at the physiological temperature of 37 °C, mimicking a surgical environment. The best sensitivity of $S = 0.023\ kPa^{-1}$ was achieved over a pressure range from 0 to 174 kPa. The performance of the pressure sensors described here show promise for use in surgical and non-invasive pressure sensing.

Contents

List of Figures

List of Tables

Chapter 1

Introduction

Pressure-sensitive devices have become very important in monitoring the health of a patient at home or at the hospital. For example, a patient might wear a device on his body to closely monitor his blood pressure; however, to make a dependable device the customer can benefit from has been a challenge to this day. Personalized devices might be needed depending on the patient's circumstances. Constraints such as sensing area, pressure ranges, and environmental conditions can be problematic when trying to match the patient to the appropriate device. Sensors, like those placed on surgical tools such as catheters and cystoscopes, have serious constraints due to the nature of minimally invasive surgeries [1]. Figure 1.1 shows a cystoscope which is a surgical instrument that allows continuous water flow. The pressure sensor must be waterproof and designed to fit a smaller area in order to be placed on the surface of the cystoscope. The healthcare provider might need to use an unconventional sensor that is not commercially available. A dependable device is challenging to fabricate because of this patient-matching limitation. Many fabrication methods involve changes in sizes and materials and tested to achieve higher sensitivity which tells the user the degree of responsiveness to changes of an external applied pressure.

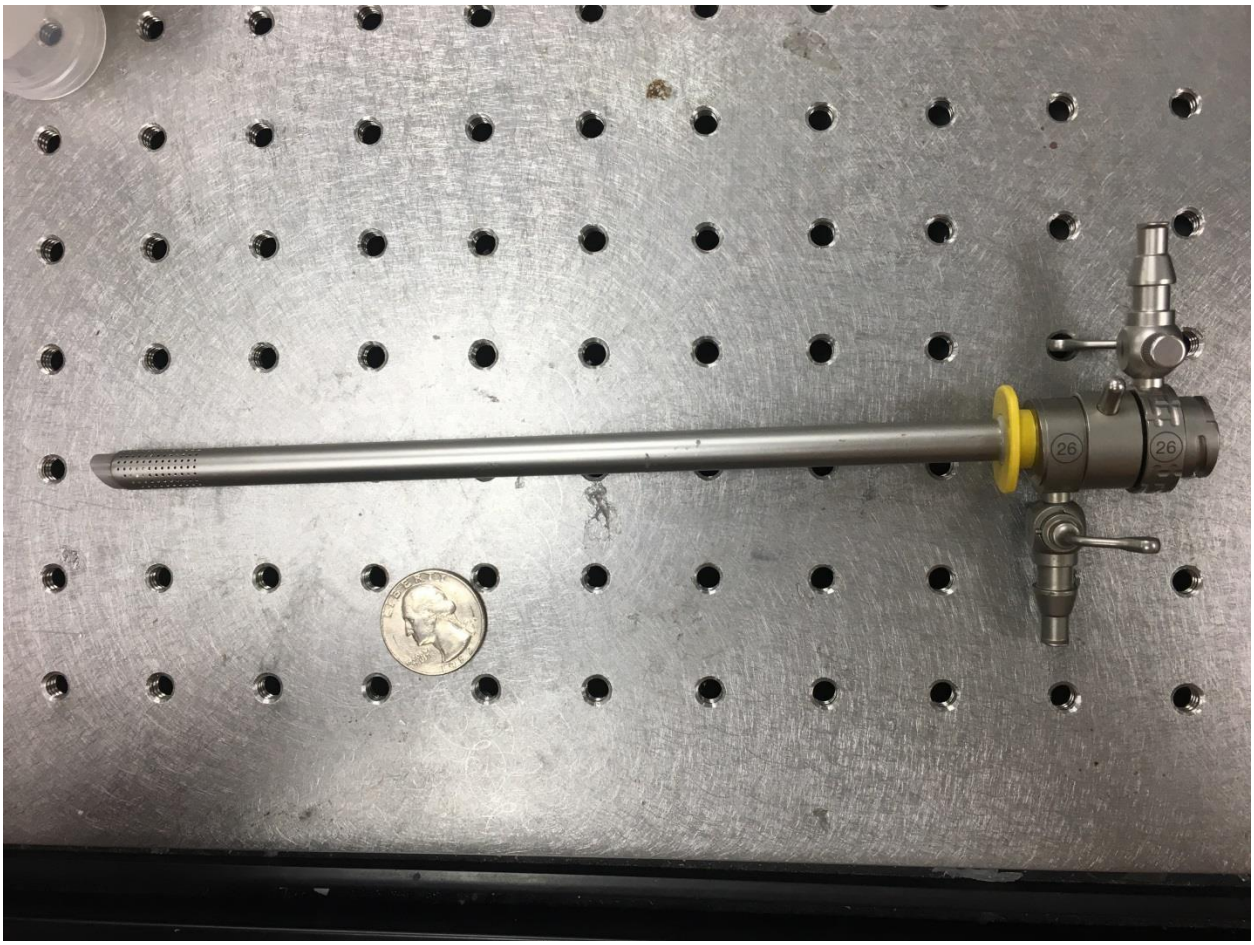

Figure 1.1: A cystoscope is a surgical tool 8.67 mm in diameter. A pressure sensor can be fabricated to fit the area constraints on the surface of the tool without disturbing the surgical procedure. The sensor can also be fabricated to maintain a low profile to maximize comfort for the patient.

Two prevalent methods used for sensing forces are made from resistive and capacitive elements [2]. Kang et al. described the advantages from capacitive pressure sensor designs as opposed to resistive pressure sensors or other principles. Those advantages include high sensitivity, low power consumption, simple design and very fast response [3]. The simple design of capacitive pressure sensors made it possible to meet specific criteria. Some devices were made using microporous dielectric layers with large capacitor plates to cover large areas in the human body [4, 5]. Chen et al. made a foot plantar pressure sensor to show the performances under

both walking and running conditions [5]. Kwon et al. made a large 12 mm x 12 mm area sensor that was used as a patch onto a human wrist and integrated in robotic fingers [4]. Other devices were made from using solid dielectric films with 3 mm x 3 mm capacitor plates to cover small areas in the human body [6]. El-Molla et al. reported a dynamic response time of less than 15 seconds for their 100-µm-thick dielectrics [7]. The dynamic response time gives important information regarding the recovery from applied pressure to the original state. The limitations from making thinner dielectrics include the durability and the amount of force applied before rupturing the dielectric layer.

Changes in the design and fabrication processes of these capacitive pressure sensors resulted in a change of overall performance in terms of sensitivity. For a pressure sensor, the sensitivity describes the change in the output signal as the applied pressure input changes. Researchers who used polydimethylsiloxane (PDMS) as their dielectric layers all used the same recipe of 10:1 base to curing agent ratio [4, 6, 7], and resulted in different sensitivities from low to high pressure ranges. El-Molla et al. was able to achieve a sensitivity of S = 0.7 pF/N at a low force of 0.15 to 0.45 N, however, the sensitivity decreased to S = 0.06 pF/N with the increase in applied force of 1 N [7]. Dinh et al. reported a sensitivity of S = 0.012 pF/N was reported at high forces applied from 0 to 6 N [6]. The sensors were fabricated to achieve a thickness of 0.66 mm, controlled by spin coating. Kwon et al. prepared the dielectric layer by a simple mixing method compared to the spin coating method [4]. Chen et al. reported a sensitivity of S = 0.01 kPa^{-1} at a pressure range of 250 kPa with a dielectric 2 mm thick and with a response time of 15 milliseconds [5]. Kwon et al. reported a higher sensitivity of S = 0.077 kPa^{-1} at a high pressure range of 250 kPa but had with a thicker dielectric of 12.7 mm [4]. They also showed a slower response time of 212 milliseconds. The results show that achieving satisfactory values for sensitivity in favorable pressure ranges both low and high has been a challenge for researchers.

This project used an uncomplicated method for fabricating microporous PDMS dielectrics with sugar. The PDMS dielectric layers involved various ratios of pre-polymer to curing agent for a different dielectric recipe that does not use a 10:1 ratio as previously mentioned above. Increasing the ratio of PDMS base agent to curing agent will change the elasticity and compressibility of the dielectric [8]. The aim is to achieve sensitivity and dynamic response times with the changes in dielectric properties. Another aim is to make a device with a low profile of 3 mm x 3 mm x 1 mm to overcome sizing constraints and minimize the discomfort of sensors placed on surgical tools.

1.1 Sensors in Healthcare

Sensors for healthcare monitoring have evolved tremendously throughout the years with a variety available for monitoring pressure, temperature, and other diagnostics. One particular development has been the increased comfort of sensors for users due to the use of flexible materials [2, 9-11]. Specifically, PDMS has become a popular material for sensors given its flexibility and its biocompatibility [9]. In addition, more complex wearable biosensors have been fabricated by merging plastic-based sensors and silicon integrated circuits to measure the detailed sweat profile in humans [10]. Sensors aiding in patient self-monitoring have facilitated healthier lifestyles by taking responsibility of their own personal diagnostics like in Figure 1.2 [4].

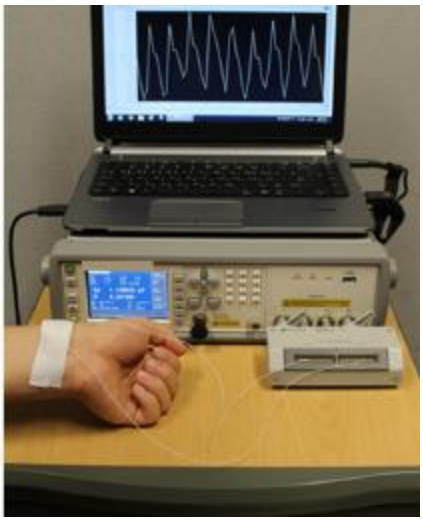

Figure 1.2: Application of a capacitive pressure sensor with a microporous dielectric layer as a wearable pressure-sensing device. Patients can use a personal computer to display the output signal of their wrist pulse signals in real-time [4].

More importantly, surgeons can benefit from using flexible sensors with low profiles in addition to their surgical tools. Operating physicians utilize instruments that often impair their capability of obtaining internal pressure information [3, 9]. Specialized sensors can assist the doctors by providing real-time analysis or visuals on the conditions inside the patient. One motivation behind this project is to make a sensor that can be placed on surgical instruments to give the doctor some feedback for a more successful surgery and minimize the risk of post-surgical complications [12]. Secondly, the project discusses the fabrication and sensitivity performance of a microporous capacitive sensor to assist in variable sensing modules. The rest of Chapter 1 discusses some examples of how elements such as resistors and capacitors can be used as pressure sensors. Chapter 2 discusses the motivation, fabrication, and performance results of the sensors. Chapter 3 discusses the conclusion and future work for medical applications.

1.2 Elements Used in Sensing Devices

1.2.1 Resistors

There have been other technologies in current, resistive, optical, vibration, and displacement based sensors used for pressure analysis [2, 3, 11]. For years, resistive commercial pressure sensors have been used for automotive, dental, and medical analysis [13]. Resistive sensors typically consist of a strain gauge bonded to a flexible polymer. The resistive element can be a polymer, conductive ink, conductive rubber, or carbon fiber [14]. Applying an external force causes a strain in the sensor and the electrical resistance of the strain gauge changes, which allows the applied force to be electrically measured [3]. Some of the limitations of the resistive sensors are due to the stiffness of packaging materials such as polyester films (Mylar), because the measurement was based on the structural deformation. To test the performance of a resistive sensor, a commercial pressure sensor (Flexiforce A201, Tekscan) was tested in parallel to the main project (Figure 1.3).

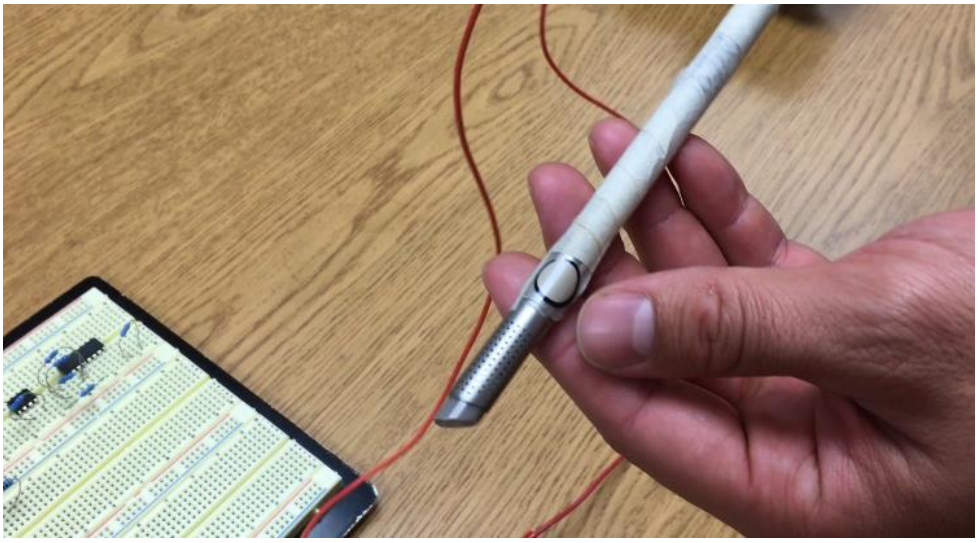

Figure 1.3: Commercial resistive pressure sensor mounted on cystoscope prior to testing.

The commercial resistive pressure sensor was also chosen because of its dimensions similar to that of capacitive pressure sensors. The sensors were made out of a polyester film known as Mylar with a thickness of 0.203 mm and a width of 14 mm. The sensing area was 9.53 mm in diameter.

Pressure sensing involves the application of an external force and a device that can transduce the pressure into a signal [2]. Pressure is defined as:

$$P = \frac{F}{A} \tag{1.1}$$

where P is pressure in Pascals or Newtons per square meter, F is the force in Newtons, and A is the sensing area.

Physicians would benefit from obtaining information about the applied pressure during a procedure such as a minimally invasive surgery (MIS). MIS will sometimes use catheters or cystoscopes as a part of the protocol [12]. Placement of the pressure sensor on the surface of one of the surgical tools would be one way of implementing the devices. Similarly, the commercial sensors were mounted on top of the cystoscope. Four different sensor lengths were chosen to be 50.8, 101.6, 152.4, and 190.5 mm. Each 14-mm wide sensor was heated to control the curvature to conform to the cystoscope, which was 8.67 mm in diameter. With the consultation from a healthcare professional, it was decided that the sensor would be tested at a pressure range of 0 to 15 kPa, because anything above that might harm the patient.

To test the performance of the resistive sensor, a drive voltage was applied to the positive end of the resistor. The output voltage was scaled up using an inverting op-amp. The data was collected to a USB Data Acquisitioning module connected to a computer. The data was displayed in LabView after pressure was applied uniformly across the sensing area of the sensor. To characterize the sensor, the sensitivity was calculated. Sensitivity can be calculated from the

response of an output signal compared to the initial load-free signal, over the change in pressure [4-8, 13, 14]:

$$S = \frac{\left(\frac{\Delta V}{Vo}\right)}{\Delta P} \tag{1.2}$$

where S is sensitivity in inverse Pascals, and V is the voltage output signal in Volts. The sensitivity was S = 0.0599 ± 0.004 kPa^{-1} over 14 trials with the measurements were within 0.00762 kPa^{-1} of one another. for pressure ranges between 0 to 15 kPa. Unfortunately, the testing of the commercial sensor had its challenges. The sensor kept peeling off the cystoscope due to the stiffness of the material. The sensor was unintentionally damaged as the sensor was being heated to conform to the cystoscope. It is suspected that the heating exceeded the operating temperature of -40 °C to 60 °C [6]. The damaged sensors showed a delayed response from the moment the external force was applied to the moment the voltage was displayed. In some tests, the output voltage remained static resulting in a zero change in voltage. The sensor would not stay conformed to the sensor for long durations and an adhesive had to be used. Multiple cycles of unpeeling and bonding the sensor on the cystoscope changed its performance, noticeable by the unchanging output voltage and the deformation of the sensor.

The commercial sensors were only water resistant, and had to be made waterproof using a thin silicone film. The cost and challenges of the commercial sensors was an incentive to move forward and test other types of pressure sensors.

1.2.2 Capacitors

Capacitive pressure sensors were selected over other sensors for reasons previously mentioned in this report, which included lower power consumption, higher sensitivity, simpler design, and faster response [2]. This type of sensor has made real-time analysis of blood

pressure possible [9]. Capacitive-based sensors have been fabricated in the size of micrometers or millimeters, to enhance their performance and increase resolution [3].

Capacitors are made of two electrodes separated by an insulator. Two conducting materials are used as the electrodes and a dielectric layer, such as air, liquid, or a polymer is used as the insulating material [15]. There are various geometries that a capacitor can have by making the electrodes in circular, helical, square, and rectangular shapes [16-19]. The capacitors can also be designed to have single or multiple layers [20]. A simple design of square parallel plate capacitor was considered in this thesis (Figure 1.4). Applying a voltage across the electrodes charges the capacitor, storing electrical energy. The amount of charge that a capacitor can store by a given voltage is an electrical property known as capacitance:

$$C = \frac{Q}{V} \tag{1.3}$$

where C is the capacitance in farad (F), Q is the charge stored on each plate in coulomb (C), and V is the voltage applied on the plates in Volts (V).

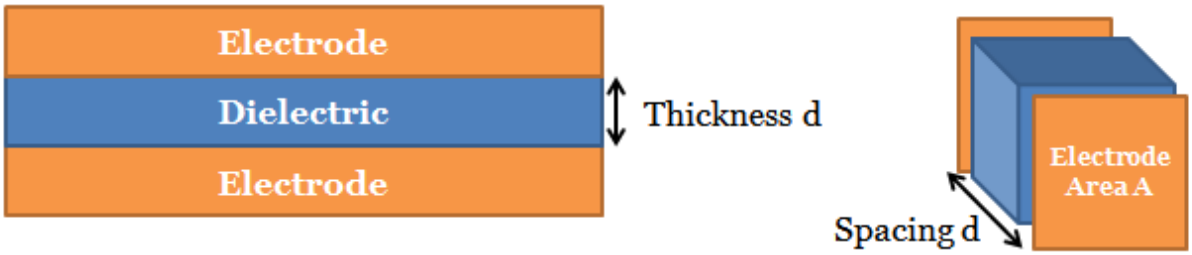

Figure 1.4: Cross-sectional view of parallel-plate capacitors. The electrodes are shown in orange with an area denoted by A. The dielectric layer is shown in blue with a thickness, or spacing between the plates, denoted by d.

The parallel plate capacitors consist of two square-plate electrodes. The electrodes are separated by a dielectric layer. As a result of the applied voltage, an electric field is generated in the space between the electrodes. The capacitance can describe the effects on the electric field. Since the electric field will weaken when the separation between the two electrodes increases we can use a different definition for capacitance that depends on the geometry and separation between the electrode plates. The capacitance of such capacitor is given by:

$$C = \frac{\varepsilon_r \varepsilon_0 \ A}{d} \tag{1.4}$$

where d is the distance between the electrodes and also known as the dielectric thickness, A is the area of the capacitive plates, ε_r is the relative permittivity or the dielectric constant, and ε_o =8.854 x 10^{-12} F/m is the permittivity of free space. If the distance decreases between the electrodes d, then the capacitance increases. If the area A increases, then the capacitance also increases. The capacitor can also have area constraints dependent on the purpose of the device. If the relative permittivity ε_r increases, then the capacitance value increases. The value for relative permittivity is limited to the type of dielectric material.

1.2.3 Microporous Capacitors

In general, the capacitor can have a dielectric made of air, liquid, or a polymer. Foam and porous elastomers have replaced solid polymers in capacitive dielectrics [21]. The fabrication of porous elastomers requires an additional ingredient mixed in to the polymer. Porous ingredients like sucrose and ammonium bicarbonate were washed out to reveal micropores in the resulting dielectric elastomer [4-5]. The microporous dielectric elastomer provided elastic compressive behavior as the pores open and close due to the external pressure. Equation 1.4 says that the decrease in separation between the electrode plates, d, allows for a greater capacitance value.

Chen et al. showed that the micropores allowed for greater displacement d which resulted in greater capacitance values and increased sensitivity of their work from S = 0.0009 kPa^{-1} without micropores, to S= 0.01 kPa^{-1} with the influence of the micropores [5]. Kwon et al. used sugar to create the micropores with sizes of 288±85 μm [4]. The effect of the change in solid to porous increased the sensitivity from S = 0.016 kPa^{-1} for solid and S = 0.077 kPa^{-1} for porous. The change in the relative permittivity contributed to the increase in sensitivity as the air, ε_r=1, in the pores are replaced with the elastomer, ε_r=2.5, during compression.

In short, resistors and capacitors are just two elements with a multitude of designs and purposes. Researches from other authors have reported that there are advantages to using capacitors as pressure sensors because of their low cost and simple design. This project has also shown that the commercial resistive sensor could be improved. For instance, the sensor should be made waterproof. The solid dielectrics in capacitor elements used as pressure sensors proved that changes in capacitances could be manipulated by changing the dimensions and materials of the devices. Combining two dielectric materials (i.e., micropores) showed to be more beneficial than having just one. It is important to continue the work in fabricating sensors that can be more of use and dependable by both patients and healthcare physicians.

Chapter 2

Microporous Capacitive Pressure Sensor Experiment

2.1 Introduction

A square-plate parallel capacitor is made into a sensor as the pressure applied to compress the dielectric, or the spacing between the plates, gives a different read out signal. One way to read the signal is to take measurements with an impedance analyzer. An impedance analyzer is an instrument that measures the impedance once it is connected to the electrodes of the device. The capacitance is then read on the impedance analyzer shown in units of Farads. The same measurement applies when the impedance analyzer is connected to a microporous capacitive sensor. The microporous capacitive pressure sensors mentioned in Chapter 1 showed performances and response times that can improve the experiences of patients and doctors in medical applications. This project aims to take another approach in fabricating the microporous capacitive sensors to increase the sensitivity of the device without sacrificing sensor dimensions and costs of materials.

2.1.1 Background and Motivation

In this thesis, an easy cost-effective fabrication method was chosen to make five microporous capacitive pressure sensors with varying mixing ratios. The motivation behind making this sensor came from a surgeon who wanted to test the performance of pressure sensors placed on the surface of surgical instruments. Patients who are critically injured, who suffer from urological problems, or who require minimally invasive surgeries might call for the use of catheters or cystoscopes [1, 12, 14, 22, 23]

Bladder catheterization, for example, involves inserting a urethral catheter to the patient to drain off urine. Water can be used to flush obstructions through which will introduce additional pressure on to the patient. The surgeon is unaware of the additional pressures due to the limited visibility and can cause tears and provoke infections in the patient. Issues in reduced invasive surgeries arise from the small incisions that reduce the degree-of-freedom during manipulation [14]. Although simple movements are no problem for a surgeon, movements like knot-tying and suturing make manipulation tasks more difficult [2]. There is also a lack of feedback from the surgical instruments to the patient's tissue that can cause tissue damage. The sensor can be used to tell the surgeon the depth of insertion, changes in applied pressures, and the duration of the applied pressures from the surgical instruments. The pressure range of interest was from 0 to 15 kPa. To put things into perspective, a commercial resistive pressure sensor was mounted on a cystoscope and tested at the pressure range.

The commercial resistive sensor was tested in laboratory dry conditions but evident damage was done to the sensor with the heating and binding on to the cystoscope. Fabricating microporous capacitive sensor was going to be more beneficial for the cause in surgical aid. The simple design of the capacitor was going to make it easy to fabricate a sensor that could overcome sizing constraints. The benefit of making a small sensor would provide comfort for the patient and overall satisfaction from the healthcare physicians. The sizes of the instrument tools

can vary and having a sensor that does not protrude would be valuable in the medical industry. Due to the nature of a surgery (e.g., MIS) the sensor would need to be tested at the physiological temperature of a human body. Temperature is not a major factor in its capacitance.

The dielectric material was chosen to be fabricated from adding PDMS with sugar. PDMS is flexible, biocompatible, and cost-effective. Granulated sugar is available and easily soluble in water for revealing the micropores. The PDMS base agent and curing agent were chosen to be mixed at different weight ratios to observe the performance in sensitivity. The hope is to increase the elasticity for an improved sensitivity with the increase in PDMS mixing ratios. With the construction of a pressure sensing device placed on surgical tools, the surgeon can get accurate feedback on the amount of pressure inside the patient, therefore, preventing any additional pressures capable of damaging the patient and shortening the recovery time.

2.2.2 Literature Review

A literature review was done to investigate recent capacitive pressure sensors. The capacitor element was chosen because it is simple to fabricate at a low cost, has a fast recovery time, and offers good sensitivity to small deflections [2].

To make a thin capacitor, the parallel plate model was chosen (Fig. 1.4). The area of the electrodes was defined by A, ε_r was the relative permittivity of PDMS, and ε_o was the permittivity of vacuum. The capacitance of the sensor decreases with the smaller area (Equation 1.4), however, the smaller area size was chosen to be able to compare the sensor to previous work [6, 7]. Another advantage of using a size of 3 mm x 3 mm meant that the sensor could fit on the tip of surgical tools such as a catheter or cystoscope. The electrodes were made of copper tape because it can be cut to any desired length and width. It has a thickness of 0.07 mm which worked better for this device because it did not compromise comfortability or flexibility to the

final design. Other work used more complicated fabrication methods to make their electrodes from carbon nanotubes or indium-tin oxide-coated poly(ethylene terephthalate) film [5, 7].

The dynamic response time gives important information regarding the recovery from applied pressure to the original state. El-Molla et al. reported a dynamic response time of less than 15 seconds for their 100-µm-thick capacitive sensors made with solid dielectrics [7]. They failed to test higher pressure ranges because their dielectric could not be compressed any further while maintaining the same recovery time. Kwon et al. reported a response time of 212 milliseconds with their 12.7-mm-thick dielectric and Chen et al. used a 2-mm-thick dielectric and reported a response time of 15 milliseconds [4, 5].

An important performance metric is sensitivity, defined in Equation 2.1 and 2.2. Sensitivity S is defined by the change in capacitance ΔC in pF divided by the change in force ΔF as well as ΔC divided by the load-free capacitance C_o divided by the change in pressure [4-7].

$$S = \frac{\Delta C}{\Delta F} \tag{2.1}$$

$$S = \frac{\left(\frac{\Delta C}{C_0}\right)}{\Delta P} \tag{2.2}$$

Researchers who used PDMS for the dielectric layer used the same recipe of 10:1 base to curing agent ratio [5- 7], and resulted in different sensitivities from low to high pressure ranges. The sensitivity reported by El-Molla et al. was S = 0.06 pF/N over a force range of 0 to 1 N They reported an increase in sensitivity to S = 0.7 pF/N at a force range of 0.15 to 0.45 N. A solid dielectric layer was used in their capacitive sensor. Although the solid capacitive sensors reported sensitivities and dynamic response time, the performances from the microporous capacitors were preferred. Chen et al. reported a sensitivity of S = 0.0009 kPa^{-1} and S = 0.01 kPa^{-1} at a pressure range of 0.33 to 250 kPa with a solid dielectric and microporous

dielectric, respectively [5]. Kwon et al. reported a higher sensitivity of S = 0.077 kPa^{-1} with a microporous dielectric compared to their solid dielectric with sensitivity S = 0.016 kPa^{-1} at a high pressure range of 30 to 130 kPa [4]. Fig. 2.1 shows their solid and microporous dielectric layers being compressed. The change in the relative permittivity contributed to the increase in sensitivity as the air, ε_r=1, in the micropores are replaced with the elastomer, ε_r=2.5, during compression.

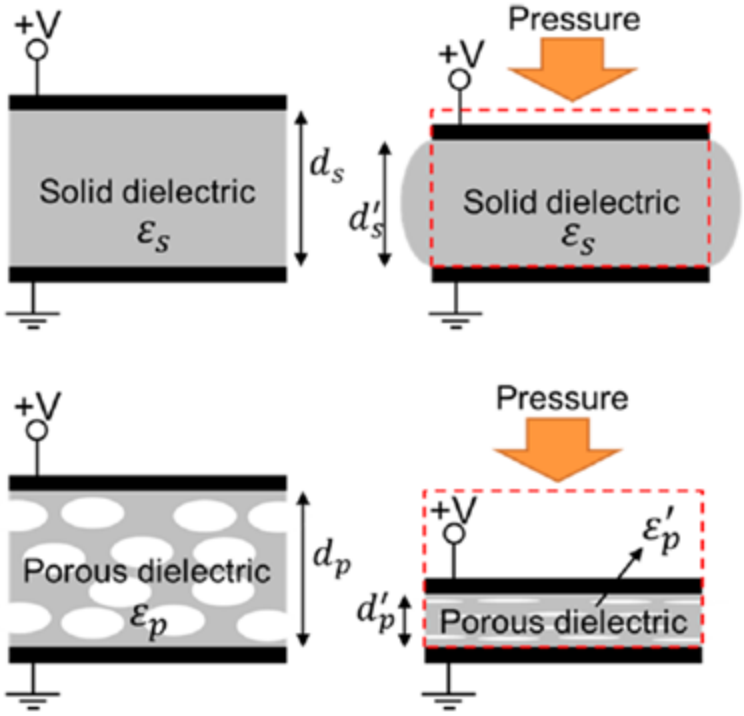

Figure 2.1: This figure reproduced from Kwon et al. [4] shows the compression of one capacitive sensor with a solid dielectric layer and one with a microporous dielectric layer. The relative permittivity of the elastomer was calculated to be ε_r=2.5. An applied pressure gave a capacitance reading and the sensitivity was measured. The influence of the micropores added two relative permittivity constants. The air pockets, with ε_r=1, allow for greater compression as the air pockets decrease. An equal applied pressure resulted in a greater capacitance reading.

PDMS was used as the dielectric material in this project, and has a relative permittivity ε_r between 2.3 and 2.8 [24]. Researchers typically use a 10:1 ratio of PDMS base agent to curing agent, but increasing this ratio makes the polymer softer, which allows for more compressibility [8]. In this work, the ratios between the pre-polymer and curing agent were changed five different times. Granulated white sugar was added to the mixture to make microporous dielectric layers. Granulated sugar is easily soluble in water and has crystal sizes ranging from 200 to 450 microns [25, 26]. The sugar crystals could be added to the PDMS mixture and then dissolved in water after the polymer has cured. The air pockets left over from the dissolved sugar crystals allows for greater compression with an external applied pressure that leads to higher sensitivity. In addition, granulated sugar is cost-effective and easily available as a household solution.

Characterization of the pressure sensors was performed at 19 °C, the ambient room temperature. The sensor with the best performing sensor was duplicated to show reproducibility. This project aims to prove that a dependable and sensitive device can be achieved using the newly created microporous PDMS dielectric of a higher mixing ratio. Another test was performed at of a physiological human body temperature of 37 °C to mimic the environment of a catheterization operation. In theory, temperature will change the dielectric constant [24] but that does not translate to direct temperature dependence in capacitive-based sensors [2].

An evenly distributed force applied to the capacitor changes the dielectric separation between the electrode plates. A force application machine was designed to achieve a uniform external applied pressure across the capacitors top electrode. Kwon et al. used an expensive force application machine ranging $400 to $1,200 (INSTRON). The accuracy of the force application depended on the mass of each free weight used. Since pressure is determined by the force per area, the force needed to be calculated to determine the pressure ranges tested. Force

is also defined as the gravity force per kilogram of mass multiplied by the mass. Since the gravity force is 9.8 N/kg, a scale was used to measure the masses in kilogram to determine the applied force. Knowing the applied force from the masses used in the force application machine (FAM), and sensing area of the pressure sensor, the applied pressure ranges were easily calculated. The pressure ranges motivated by the minimally invasive surgeries were 0 to 15 kPa, however, the limit of the force application machine was up to 174 kPa. The decision was made to test the pressure sensors in a higher pressure regime to better compare with other work. The testing done at other pressure ranges might broaden the use of these sensors with their promising performances.

The following sub-chapters go into more detail of the design, fabrication, and results. A literature review was done and this work showed promising results when compared to other work. The aim was to fabricate a capacitor with a low profile that was comparable to commercial and lab-made sensors.

2.2 Design

The capacitive sensors were designed to have a total of three layers: two electrodes and one dielectric layer in between the electrodes. Copper tape electrodes were chosen for the design because they provided an adhesive to the dielectric layer. The electrodes were designed with an area of 3 mm x 3 mm. For testing purposes, the copper tape could be cut to a desired length to make better connections to the testing setup on impedance analyzer (HIOKI IM3570). The dielectric layers were made of PDMS base, PDMS curing agent, and granulated sugar. The ratios from the PDMS base and curing agent were changed to make five different dielectrics (Sylgard 184, Dow Corning). Previous work had included a 10:1 ratio, or 10%, of PDMS base agent to

curing agent. A decision was made to increase this ratio, equivalent to decreasing percentage, to 11, 13, 15, 19, and 31 of base to 1 of curing agent. The white granulated sugar was added to make the micropores. White table sugar was chosen instead of another material (i.e., ammonium bicarbonate) because it was cost effective, it can be found in most households and recycling unused products can help reduce waste; making a case for using sugar for more than just a food sweetener. [5]

The sensor area and thickness sizes were determined by a few factors; per doctor request, ease of handling, and comparison to previous work [6, 7]. The size of 3 mm x 3 mm x 1 mm meant that the sensor could fit on the tip of surgical tools such as a catheter or cystoscope. Capacitance also decreases with larger dielectric thickness and the doctor requested a thin sensor to achieve comfortability for patients. The force application machine design was based on three factors; the ability to hold enough weights, to cover the sensing area, and to be economical.

2.3 Fabrication

2.3.1 PDMS Base to Curing Agent Ratios

Five PDMS dielectric layers were prepared by mixing PDMS base agent and curing agent (Sylgard 184, Dow Corning) in a weight ratio of 11:1, 13:1, 15:1, 19:1 and 31:1respectively (Figs. 2.2 and 2.3). Each layer was mixed for five minutes in Petri dishes to ensure uniformity. As a result of mixing, air bubbles were formed (Fig. 2.4). The percentages were chosen prior to converting to ratios; e.g. a 10:1 ratio corresponds to a 10% base to curing agent recipe and results in a harder PDMS. The percent was decreased and the above were the corresponding ratios.

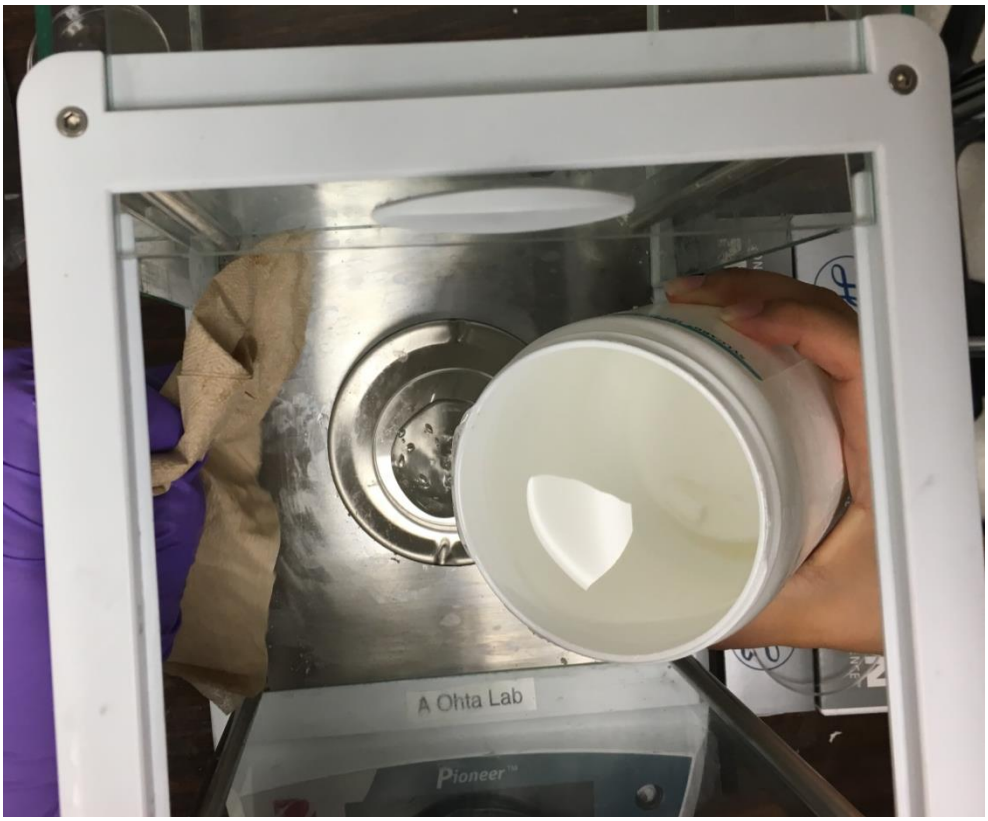

Figure 2.2: The PDMS base agent was added to the Petri dish. The Petri dish was located on top of a scale to record the weight in grams. From this, the weight of PDMS curing agent was calculated. The PDMS base is a clear viscous liquid.

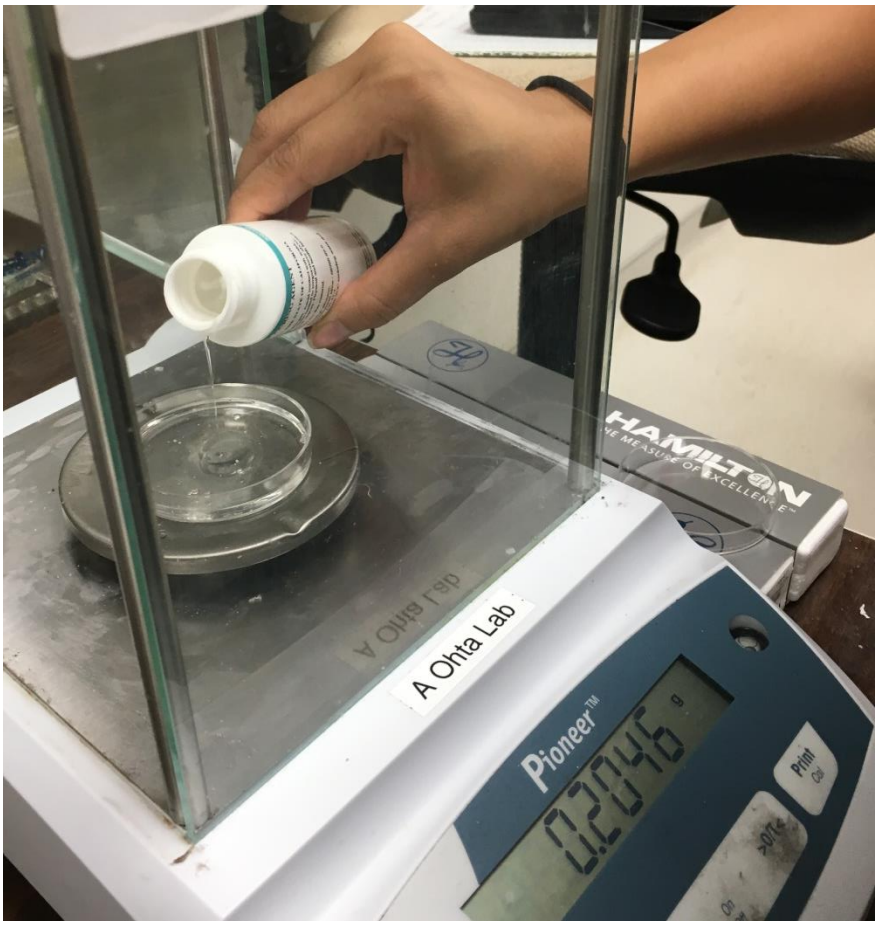

Figure 2.3: The PDMS curing agent was added to the Petri dish to achieve the desired weight ratio. The curing agent is a clear liquid and is responsible for giving PDMS the solid structure after curing [27].

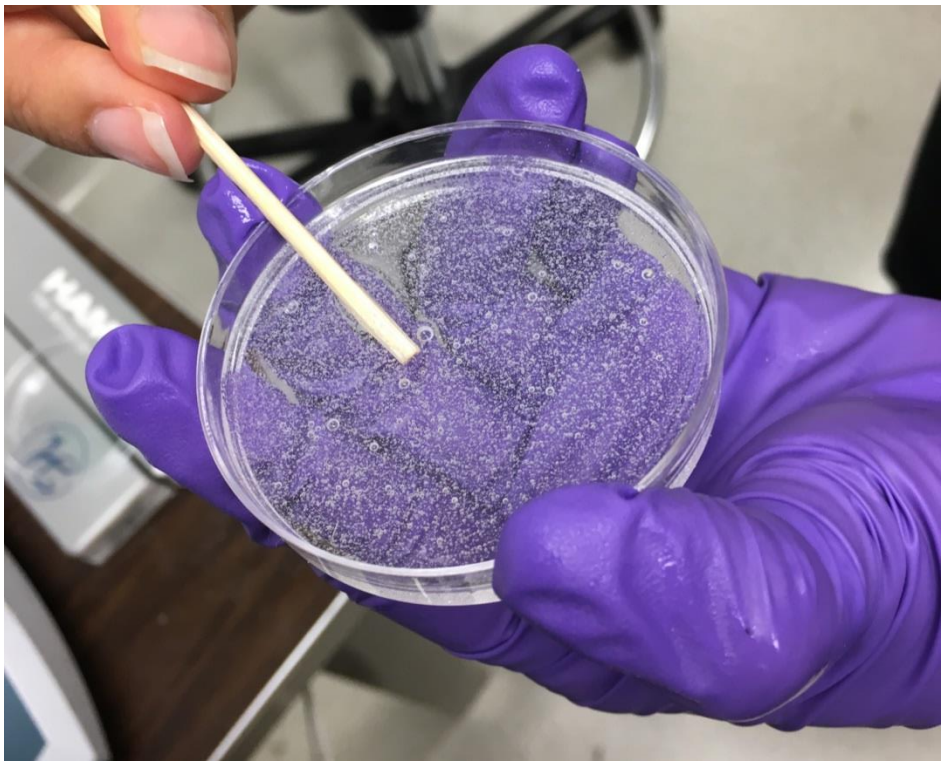

Figure 2.4: As a result of mixing the PDMS base agent and curing agent for a total of five minutes, air bubbles formed inside the uncured solution.

2.3.2 Granulated Sugar

The granulated sugar (C&H) was added in the five Petri dishes that contained the uncured PDMS mixture (Fig. 2.5). As the sugar submerged to the bottom of the Petri dish, addition of the sugar continued until the entire solution was filled with sugar. The Petri dishes were degassed for 30 minutes in a vacuum chamber to remove the air bubbles formed during the mixing. Then, the Petri dishes were transferred to an oven and cured at 75 °C for 60 minutes. They were left overnight at room temperature before handling. The dielectric layers were removed from the petri dishes and washed in warm water to remove excess sugar granules not cured with PDMS. Each dielectric layer was cut into quarter pieces for better handling. The pieces were shaken in warm water for five minutes until all the sugar inside the PDMS was

dissolved and the microporous dielectric layers were revealed (Fig. 2.6). To ensure that all the sugar crystals were dissolved, the PDMS was cut and repeatedly rinsed with water. They were left to dry overnight at room temperature.

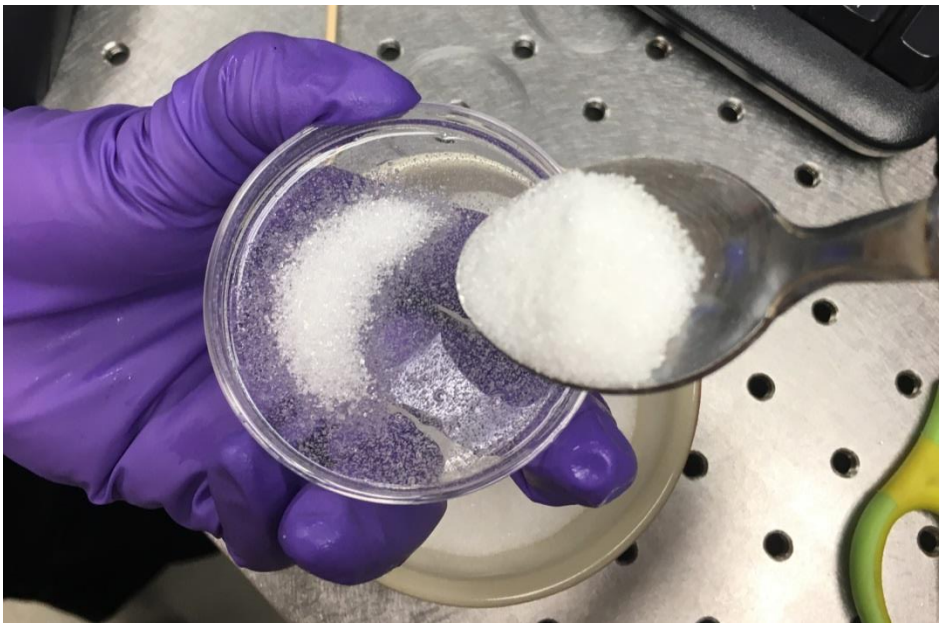

Figure 2.5: The addition of white granulated sugar to the uncured PDMS was done until the solution was completely filled with sugar. After curing the PDMS dielectric, the sugar crystals were dissolved to reveal the micropores.

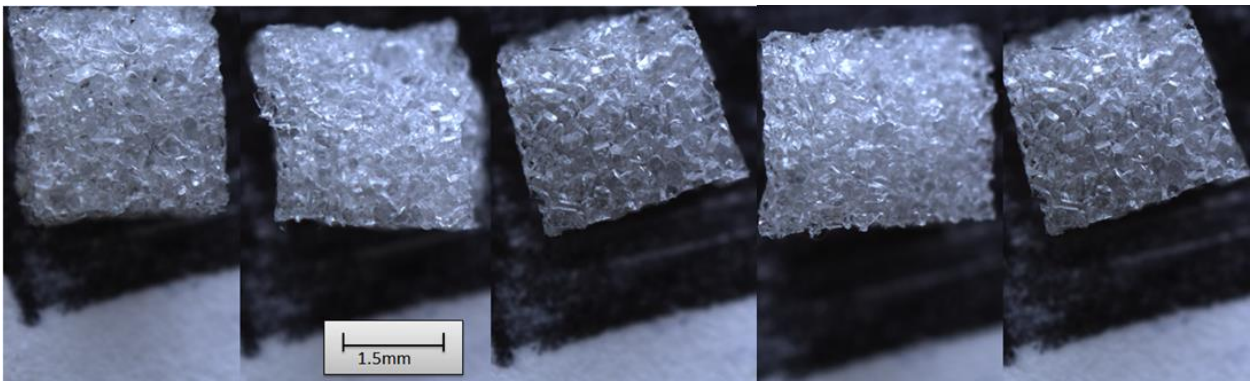

Figure 2.6: The fabricated microporous PDMS with (a) 31:1 base agent to curing agent ratio (b) 19:1 base agent to curing agent ratio (c) 15:1 base agent to curing agent ratio (d) 13:1base agent

to curing agent ratio and (e) 11:1 base agent to curing agent ratio. Notice their foam-like appearance, which provides increased flexibility and responsiveness to an applied pressure.

The micropores were observed using a microscope (Fig. 2.7). Using ImageJ, the average lengths of the micropores were measured by converting the pixel sizes to micrometers. The micropore sizes were observed to be 358 ± 68 μm, 289 ± 135 μm, 369 ± 128 μm, 451 ± 200 μm and 347 ± 274 μm for the 31:1, 19:1, 15:1, 13:1, and 11:1 PDMS mixing ratios, respectively.

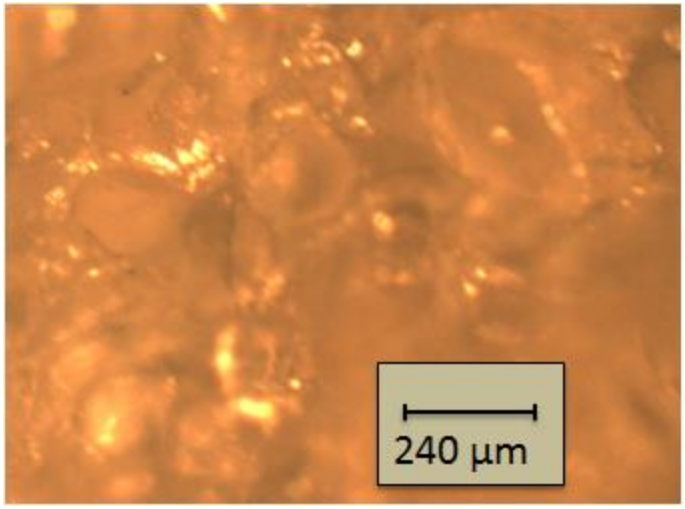

Figure 2.7: The 31:1 PDMS mixing ratio observed under a microscope. The microporous structure was determined by the paying close attention to the outlining of the unfocused filling. The Feret diameter, or the average of the longest length in the x-y plane, for each dielectric was measured with ImageJ.

2.3.3 Cutting and Mounting Sensor

Each piece of microporous dielectric was cut into 3 mm x 3 mm squares. After being cut they were sliced to achieve a thickness of 0.9 mm. The size was measured by a digital caliper. The copper tape electrodes were cut to match the 3 mm x 3 mm microporous dielectric layers. The thickness of the copper tape was 0.07 mm. Each dielectric layer was placed in between the

electrode layers to complete the fabrication of the microporous capacitive pressure sensor with dimensions of 3 mm x 3 mm x 1 mm. The sensors were connected with a micro-positioner (Fig. 2.8). The electrodes were connected to the impedance analyzer.

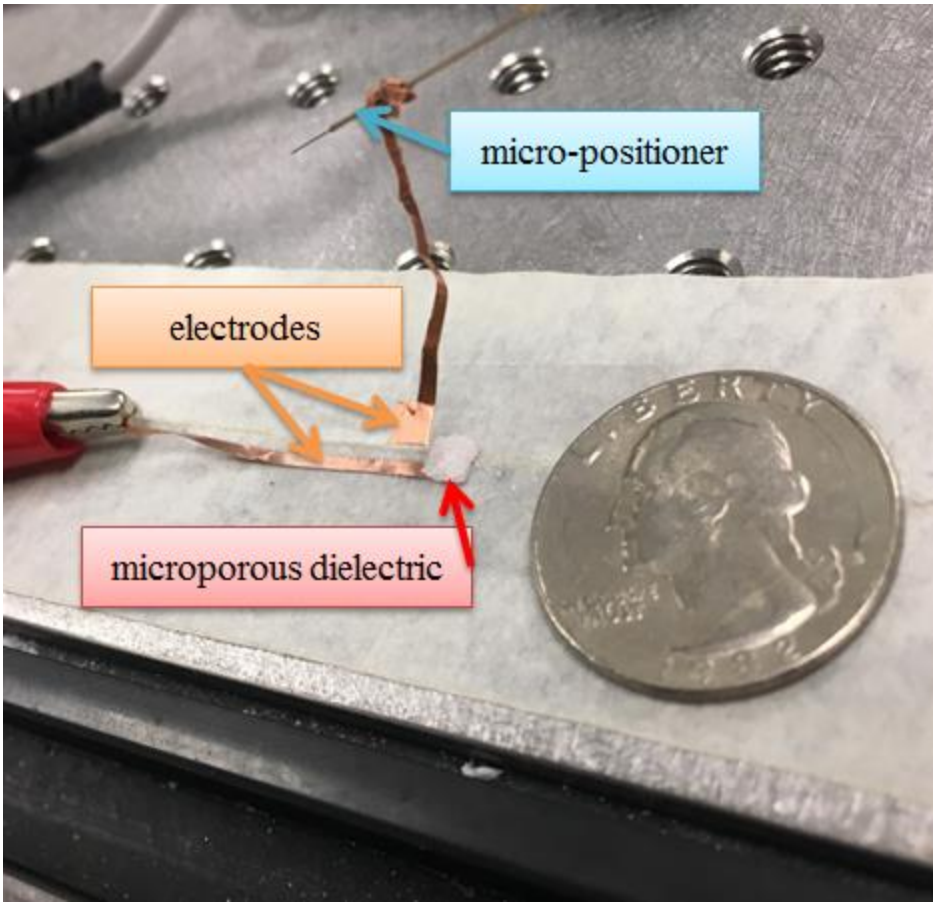

Figure 2.8: Microporous capacitive pressure sensor made of two copper electrodes and a dielectric. A quarter was placed for a size comparison. The top electrode is connected to a micro-positioner. The micro-positioner was used to keep the top electrode stable as any movement to the tiny device ejected into the air.

2.3.4 Force Application Machine

A cost-efficient and time-saving force-application machine (FAM) was designed using a scale, weights, a stand, and a pipette. The materials used were found typical in a microfluidics laboratory if one chose to replicate the device. A lab made FAM was more convenient to make rather than buying an expensive machine that ranges from $400 to $12,000. The pipette was held by a stand. Once the testing began, the stand was loosened to release the pipette and allow the force of the pipette to cover the whole area of the sensor. A laboratory scale was used to weigh the different masses. A total of 50 weights were used totaling in0.16 kilograms to achieve the pressure range of 0 to 174 kPa. Researchers had defined the low, medium, and high pressure ranges to be 0-10 kPa, 10-100 kPa and greater than 100 kPa, respectively [3]. The opportunity was taken to cover a wide pressure range. The limit of the FAM was 174 kPa and a decision was made to test up to this pressure.

2.4 Experiment

The experiment was performed at 19 °C which was the ambient temperature inside the microfluidics laboratory. One at a time, the microporous capacitive sensors were mounted on the stage and connected to the impedance analyzer. Fig. 2.9 shows the complete set up for the experiment. The FAM was carefully placed next to the sensor so that the pipette could be located above of the sensor. The pipette was secured by the stand and released when the sensor was ready for testing. The impedance analyzer (HIOKI IM3570) was switched on. It is capable of high-speed sweep measurements of frequencies and signals with 10 kHz, 100 kHz, and 1 MHz, and 1 V_{rms} amplitude ac signals. High-speed measurement of 0.5 ms is possible at 100 kHz. The impedance analyzer functions as an LCR meter with a touch panel displaying measurement conditions. Capacitance measurement condition was chosen for this experiment. Data collecting

began with the load-free capacitance value. Then, one by one the weights were placed inside the pipette. The applied pressure on the sensor resulted on the compression of the dielectric and a change in capacitance value. The pressure range tested was between 0 to 174 kPa. Each sensor was tested using the same weights following the same order. The test was repeated five times at each frequency sweep. The frequencies were chosen for a better comparison with other research mentioned throughout this project [4-7].

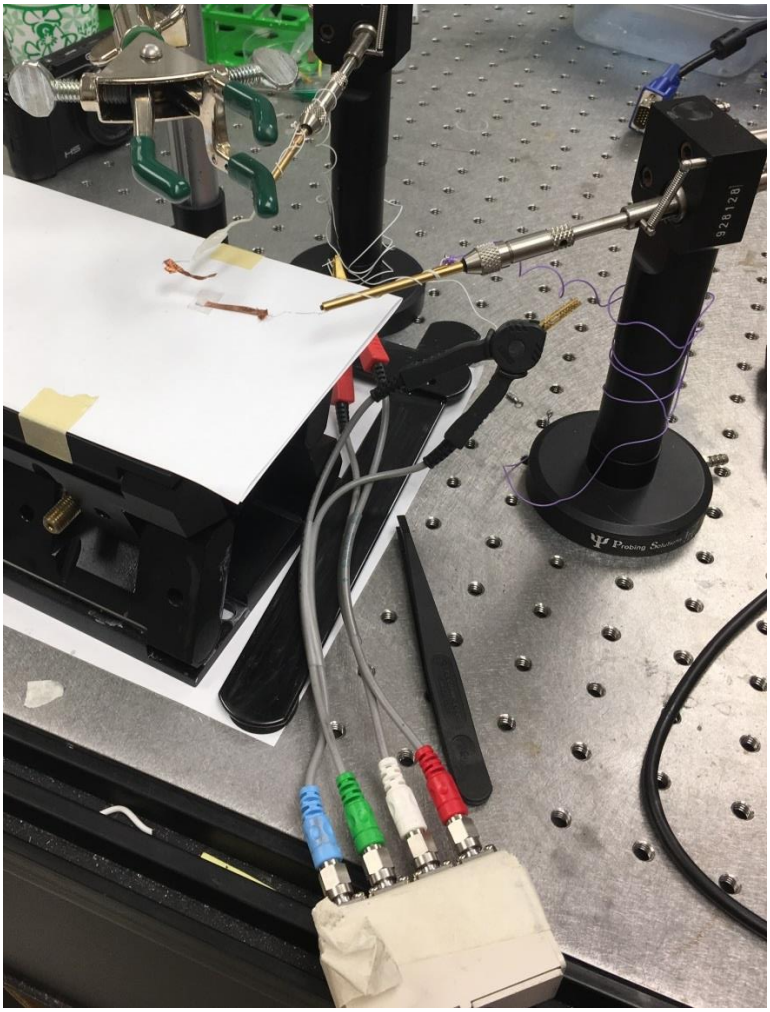

Figure 2.9: The final set up of the FAM, microporous capacitive pressure sensor, micro-positioners, and impedance analyzer connections. The sensor was small and delicate in comparison to the testing equipment. Careful attention was put to ensure the sensor was not ejected or displaced from the stage.

2.4.1 Pressure Test

The impedance analyzer was chosen to characterize each sensor. The device is an impedance measuring instrument with a high degree of accuracy. Speed was important for time-saving efforts since the test required 50 weights added into the pipette. The pressure test was performed on five sensors with varying PDMS mixing ratios of 31:1, 19:1, 15:1, 13:1, and 11:1. Repeating the test five times resulted in 260 capacitance measurements per sensor. Since the frequency sweep was done with 10 kHz, 100 kHz, and 1 MHz, a total of 1,300 measurements were recorded. The capacitance measurements were read on the LCD display. First, the unloaded capacitance value, C_o, was recorded. Next, the FAM was used to uniformly distribute the pressure s. The sensitivities were calculated using Equation 2.1 and Equation 2.3. Table 2.1 shows the highest sensitivity values for the 31:1, 19:1, 15:1, 13:1, and 11:1 PDMS mixing ratios which were S = 0.0107 kPa^{-1}, S = 0.0173 kPa^{-1}, S = 0.00298 kPa^{-1}, S = 0.00176 kPa^{-1}, and S = 0.00669 kPa^{-1},respectively.

Ratio of PDMS	S at 10 kHz [kPa^{-1}]	S at 100 kHz [kPa^{-1}]	S at 1 MHz [kPa^{-1}]
31:1	0.00899±0.0002	0.00910±0.0001	0.01070±0.0001
19:1	0.0164±0.0001	0.0167±0.0001	0.0173±0.0001
15:1	0.00298±0.0005	0.00275±0.0001	0.00262±0.0001
13:1	0.00176±0.0001	0.00161±0.0001	0.00122±0.0001
11:1	0.00534±0.0001	0.00530±0.0001	0.00669±0.0001
Ratio of PDMS	**S at 10 kHz [pF/N]**	**S at 100 kHz [pF/N]**	**S at 1 MHz [pF/N]**
31:1	0.137±0.004	0.135±0.004	0.131±0.004
19:1	0.284±0.001	0.280±0.001	0.275±0.001
15:1	0.101±0.003	0.0920±0.002	0.0837±0.002
13:1	0.0200±0.0001	0.0175±0.0001	0.0132±0.0001
11:1	0.0568±0.0001	0.00545±0.0003	0.0486±0.0003

Table 2.1: Two sensitivity measurements for five sensors at 19°C measured at 10 kHz, 100 kHz, 1 MHz, and 1 V_{rms} AC signal. The results of the pressure test show a larger sensitivity value for the 19:1 PDMS mixing ratio when compared to the rest.

The sensitivities were also plotted (Figs. 2.10 and 2.11) to better represent the values in Table 2.1. Both figures show that the highest sensitivity was a result of the 19:1 PDMS mixing ratio. The pressure test also involved recording the dynamic response time for the dielectric layers. A high-speed camera was used to measure the dynamic response time. The response time showed the time it took for the porous dielectric to decompress after an external pressure was applied. The average response times were calculated to be 1.0 ± 0.58 seconds, 0.29 ± 0.17 seconds, 1.5 ± 0.02 seconds, 0.24 ± 0.11 seconds, and 0.10 ± 0.03 seconds for the 31:1, 19:1, 15:1, 13:1, and 11:1 PDMS mixing ratios, respectively.

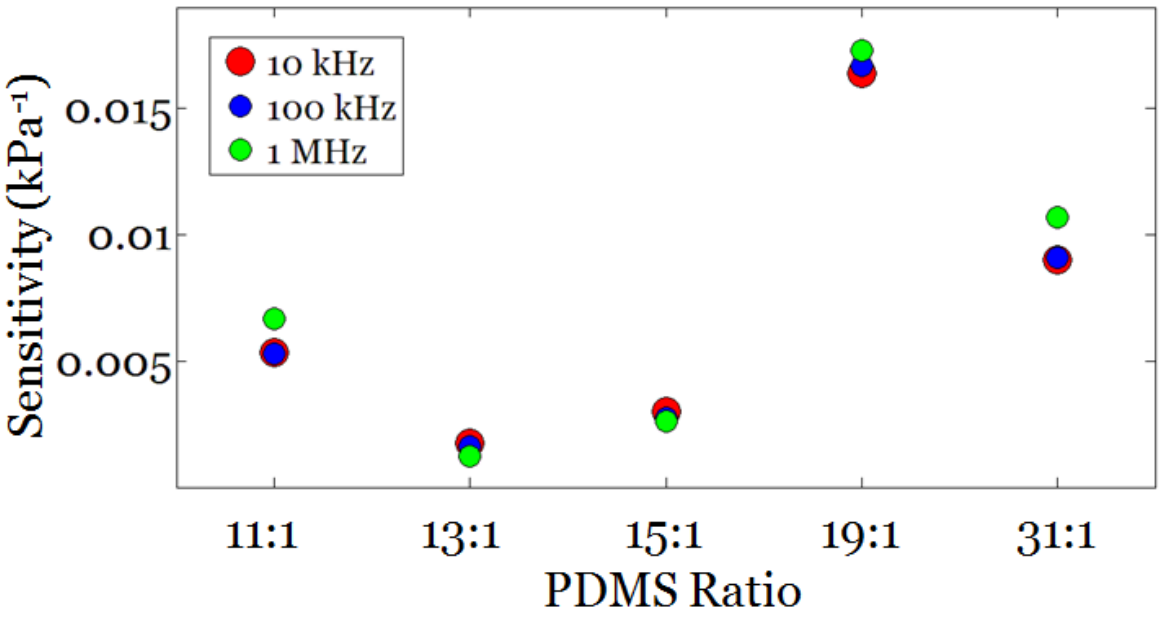

Figure 2.10: Sensitivities (measured in kPa^{-1}) for all the PDMS ratios at 19 °C. The legend indicates the measurement frequency. Notice here that the two highest sensitivities resulted from the 31:1 and 19:1 PDMS ratios with S = 0.0107 kPa^{-1} and S = 0.0173 kPa^{-1}, respectively.

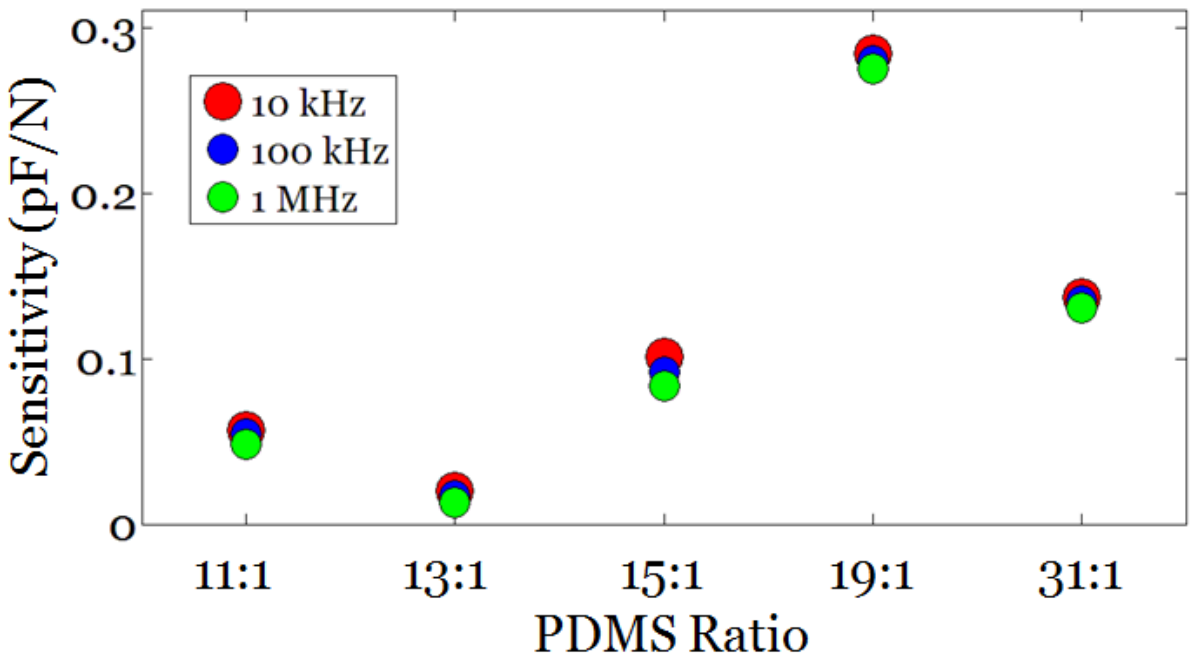

Fig 2.11: Sensitivities (measured in pF/N) for all the PDMS ratios at 19 °C. The legend indicates the measurement frequency. Notice here that the 19:1 PDMS ratio was the sensor with the highest sensitivity of S = 0.284 pF/N compared to all the other sensors. The sensor with 31:1 PDMS ratio had the second highest sensitivity of S = 0.137 pF/N.

2.4.2 Reproducibility Test

The sensor with the highest sensitivity, which was the one that used 19:1 PDMS mixing ratio, was reproduced in a total of four batches, A, B, C, and D. The pressure test from 0 to 174 kPa was performed in the same laboratory temperature of 19 °C. The results, described later in more detail, proved that the 19:1 PDMS ratio was reproducible. The calculated average sensitivity for the four different batches was calculated to be S = 0.0183 ± 0.001 kPa^{-1}.

2.4.3 Pressure Test in Surgical Environment

The sensor that used 19:1 PDMS mixing ratio, sensor A, was also tested at a temperature of 37 °C, the average physiological temperature of the human body, to mimic the environment of a minimally invasive surgery. The tests were repeated over a pressure range from 0 to 174 kPa. The nature of a minimally invasive surgery was the motivation behind this test. The average physiological temperature of the human body is 37 °C. According to the doctor, the human body can fluctuate ±1 °C during operations therefore it was determined that only once temperature test of 37 °C was necessary. A heater and thermometer were selected for achieving this temperature. The microfluidics laboratory had a thermostat that was placed directly in front of the sensor and checked regularly to maintain a temperature of 37 °C. The increase from 19 °C to 37 °C resulted in an increased sensitivity: a 28% increase with S = 0.023 kPa^{-1}. The experimental results showed changes in overall performance for the 19:1 PDMS ratio (Fig 2.12).

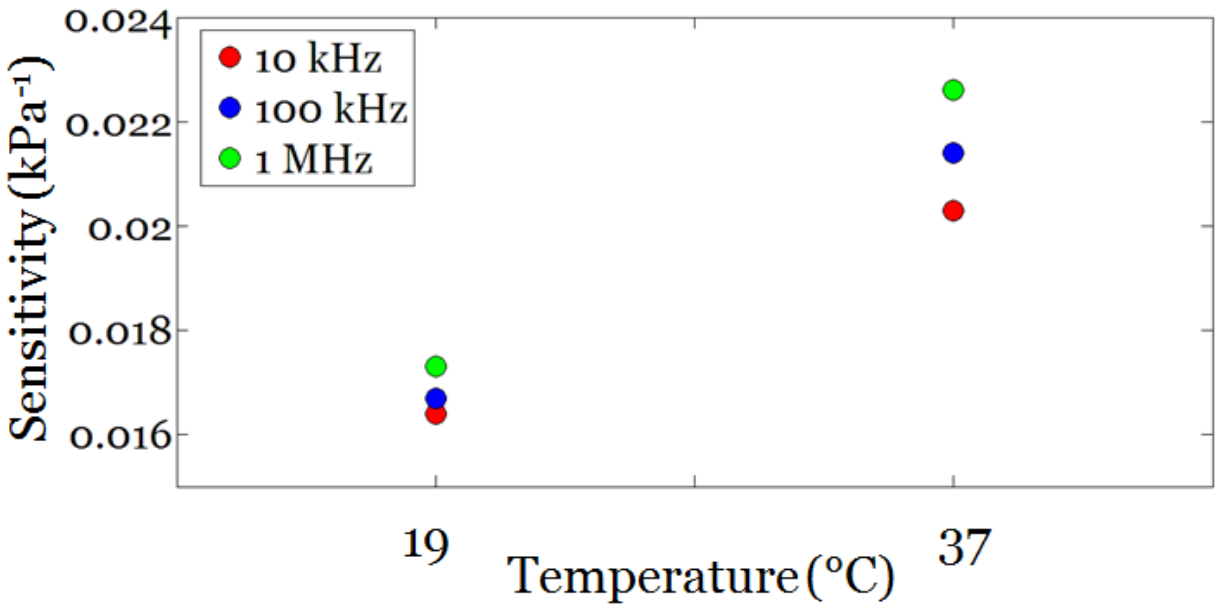

Figure 2.12: Sensitivities (measured in kPa^{-1}) for the 19:1 PDMS ratios, sensor A, at 19 °C and 37 °C. The legend indicates the measurement frequency. Notice here that the performance of the same sensor changed in the presence of a warmer environment.

Overall, the experiment was successful because the pressure test showed changes in compressibility in the five sensors with varying PDMS ratios. The capacitive pressure sensors showed promising recovery times with the pressure tests. The sensor with the highest sensitivity, which was the one that used 19:1 PDMS mixing ratio, was fabricated in different batches with reproducible properties. Sensor A was also tested at a temperature of 37 °C and showed promising sensitivities for the use in a surgical environment.

2.5 Results

2.5.1 Nineteen Degrees Celsius

Characterization for the pressure sensors was performed at 19 °C, the ambient laboratory temperature. The capacitance of each sensor was measured using 10 kHz, 100 kHz, and 1 MHz ac signals with an amplitude of 1 V_{rms}. The changes in capacitance for the pressure sensors were measured over a range of 0 to 174 kPa. First, the unloaded capacitance value, C_o, was recorded. Next, the FAM was used to uniformly distribute the pressures. Finally, the changes in capacitance over the initial capacitance was calculated and plotted versus the change in pressure (Figure 2.13). The experiment with various PDMS mixing ratios showed that the increasing PDMS base agent to curing agent ratio did result in elastic properties given by the slopes of the graph [21]. The data points did not start at zero because the initial change of capacitance is zero with no applied pressure so it was decided that including it had no significance in the data interpretation.

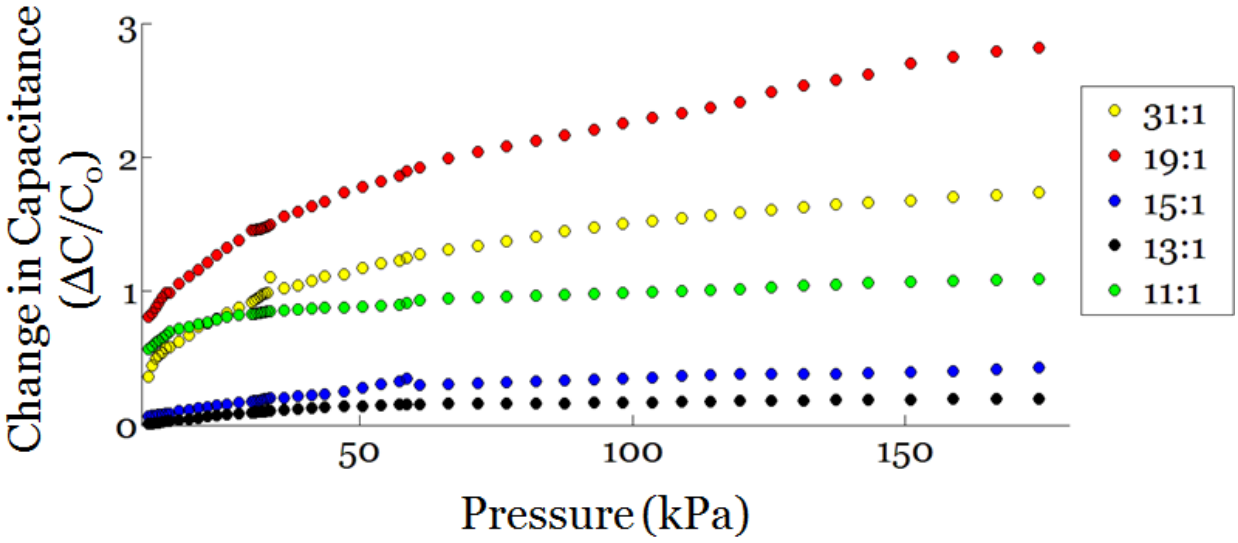

Figure 2.13: The results showed the change in capacitance (measured at 1 MHz) for all PDMS mixing ratios at 19°C, the ambient room temperature, at a pressure range from 0 to 174 kPa. The legend indicates ratios of PDMS base agent to curing agent. The red and yellow slopes corresponded to the higher mixing ratios of 19:1 and 31:1, respectively. The red and yellow slopes showed the highest changes in capacitances. The green slope corresponded to the 11:1 PDMS mixing ratios. Although not apparent, the green, blue, and black slopes were quite similar. It was suspected that the slight thickness variations between dielectrics led to the changes in initial capacitance values. A thicker dielectric would result in a smaller initial capacitance but the overall slope resulted from the compressibility of the sensor.

The sensors that used 31:1 and 19:1 PDMS mixing ratios have a higher slope than the sensors with 15:1, 13:1, and 11:1 PDMS mixing ratios. The higher slopes were from the result of the change in capacitance with the addition of applied pressure. Figures 2.11 and 2.12 illustrated the sensitivities for the five sensors represented in Table 2.1. The best sensitivity values for the 31:1, 19:1, 15:1, 13:1, and 11:1 PDMS mixing ratios which were S = 0.0107 kPa^{-1}, S = 0.0173 kPa^{-1}, S = 0.00298 kPa^{-1}, S = 0.00176 kPa^{-1}, and S = 0.00669 kPa^{-1}, respectively. Initially, it appeared that the 11:1 PDMS ratio had sensitivity comparable to the 31:1 PDMS ratio and the 19:1 PDMS

ratio, but a closer look at Table 2.1 shows otherwise. It was suspected that the slight thickness variations between dielectrics led to the changes in initial capacitance values making the sensor with 11:1 PDMS mixing ratio appear to have greater changes in capacitances than the sensor with 31:1 PDMS mixing ratio.

The micropores added elastic properties and contributed to the fast dynamic response time of the dielectrics. The dynamic response time showed the time it took for the porous dielectric to decompress after an external pressure was applied. The average response times were calculated to be 1.0 ± 0.58 seconds, 0.29 ± 0.17 seconds, 1.5 ± 0.02 seconds, 0.24 ± 0.11 seconds, and 0.10 ± 0.03 seconds for the 31:1, 19:1, 15:1, 13:1, and 11:1 PDMS mixing ratios, respectively. There was no apparent trend from the response time to the PDMS mixing ratios. The pore sizes were observed under a microscope to be 358 ± 68 μm, 289 ± 135 μm, 369 ± 128 μm, 451 ± 210 μm, and 347 ± 274 μm for the 31:1, 19:1, 15:1, 13:1, and 11:1 PDMS mixing ratios, respectively. There was no apparent trend from the micropore sizes to the PDMS mixing ratio. After analyzing the performances from the sensors using various PDMS base agent to curing agent mixing ratios, it was concluded that the 19:1 PDMS mixing ratio showed promising results in sensitivity and response time and needed further investigation.

The reproducibility test was decided on the sensor that used 19:1 PDMS mixing ratio because of its higher sensitivity. The sensors were labeled as A, B, C, and D and were fabricated in separate Petri dishes. The slopes were similar and with confidence it was determined that the sensor was reproducible (Fig. 2.14). Sensor D had a greater change in capacitance than sensor A in the start as well as in the end of the applied pressure test. An average sensitivity of S = 0.0183 ± 0.001 kPa^{-1} was calculated.

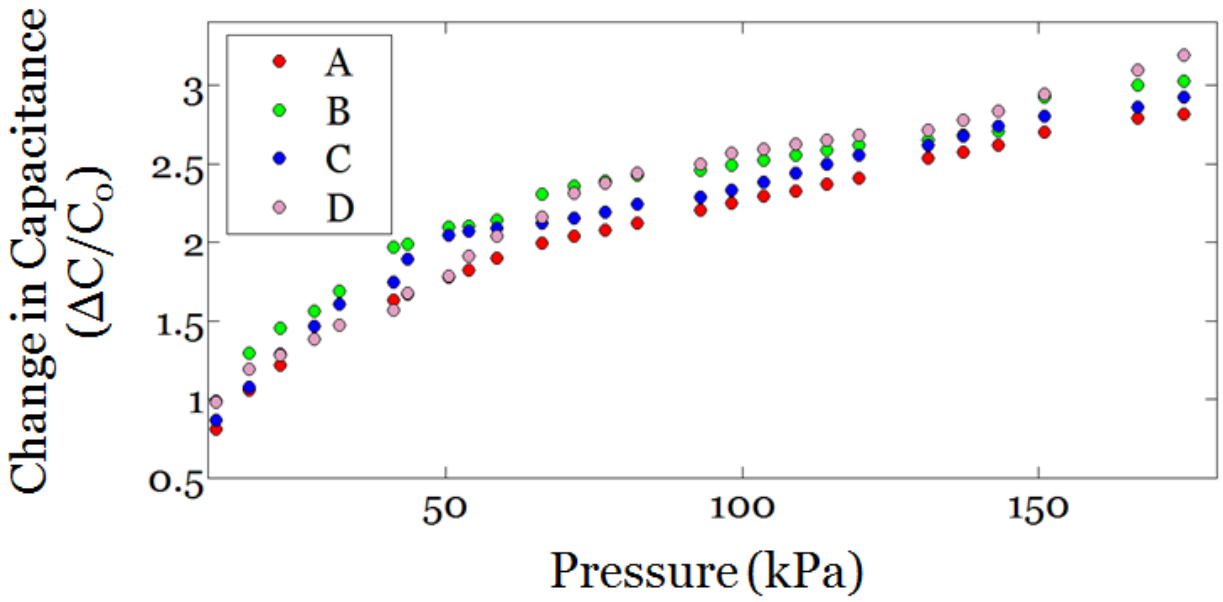

Figure 2.14: The results showed the change in capacitance (measured at 1 MHz) for the 19:1 PDMS mixing ratios at 19°C, the ambient room temperature, at a pressure range from 0 to 174 kPa. The legend indicates ratios of PDMS base agent to curing agent. Notice how the slopes have similar behavior. The initial data points and final data points follow the same trend where sensor D has a greater change in capacitance than sensor A in the start as well as in the end of the pressure test.

The following calculations were made to determine the effective permittivity from the combination of the dielectric material and the micropores. To find the effective permittivity, the fractional volume for the micropores, the relative permittivity of air, and the relative permittivity of PDMS had to be known [4, 28]. The theoretical capacitance value and the effective permittivity are defined as Equation 2.3 and Equation 2.4.

$$C = \varepsilon_0 \varepsilon_{effective} \frac{A}{d} \tag{2.3}$$

$$\varepsilon_{effective} = (1 - f_v)\varepsilon_{PDMS} + f_v \varepsilon_{air} \tag{2.4}$$

The constants ε_0, A, and d are known. The difference in spacing between the plates, d, gave out an output capacitance reading. The theoretical effective permittivity was calculated with the provided information on fractional volume f_v of the porous material. The fraction can only range from 0 to 1. Kwon et al. measured the porosity volume fraction to be 0.628 with their reported average micropore size = 288 ± 85 μm [4]. The average pore sizes measured for sensor A was 289 ± 135 μm. As an approximation, 0.6 was used as the fractional volume of the micropores in this work. The relative permittivity of air is ε_{air} = 1 and the relative permittivity of PDMS was known to be ε_{PDMS} = 2.66 when measured at 1 MHz [27]. Using Equation 2.4, the effective permittivity was calculated to be $\varepsilon_{effective}$ = 2.2. If the fractional volume of the micropores is 0.5, then the effective permittivity is $\varepsilon_{effective}$ = 1.83., and if the fractional volume is 0.4, then $\varepsilon_{effective}$ = 1.46.

Using the data from sensors A, B, C, and D during their initial capacitance where d = 0 when no pressure was applied, the average experimental effective permittivity was solved using Equation 2.3. The effective permittivity was calculated to be $\varepsilon_{effective}$ = 1.825 ± 0.051. The results here correspond to the porosity of 50% considered above. Figure 2.1 shows the effective permittivity changes during compression. Since half of the material was PDMS and the other half was air without compression, the influence due to the relative permittivity of air will no longer be a factor after the dielectric thickness reaches a thickness of d/2. To verify this, the effective permittivity was calculated using the thickness d/2 and the corresponding average capacitance value. The pressure applied during this compression was 95 kPa. The effective permittivity was calculated to be $\varepsilon_{effective}$ = 2.59 ± 0.009. During compression, the air pockets decreased and the effective permittivity increased. The volume fraction was calculated to be 0.042 for the microporous. The results show that not all the pockets were void of air at half of the compression but it was significant enough to change the effective permittivity. Figure 2.14

shows the slope increasing even after the micropores were void of air due to compression. The capacitance output values depend on the value of the effective permittivity and not just the dielectric compression.

The results for the pressure tests at 19 °C showed promising sensitivity and reproducibility for the dielectric with a 19:1 PDMS base agent to curing agent ratio. Sensor A performed with a sensitivity of S= 0.0173 kPa^{-1}. The sensor showed a dynamic response time of 0.29 ± 0.17 seconds. The dynamic response time of the sensor will be able to give the surgeon accurate feedback every 0.29 seconds an external pressure is applied and removed. The average pore sizes measured for sensor A was 289 ± 135 μm. The influence of the micropores and PDMS led to an effective permittivity of 1.825 ± 0.051. The sensor showed it was compressible and sensitive enough to be further investigated for this project.

2.5.2 Thirty-Seven Degrees Celsius

The reproducibility test on the sensor that used 19:1 PDMS mixing ratios led to the following performance test mimicking a MIS environment. Characterization for the pressure sensors was performed at 37 °C. The capacitance of each sensor was measured using 10 kHz, 100 kHz, and 1 MHz ac signals with an amplitude of 1 V_{rms}. The change in capacitance for the pressure sensors was measured over a range from 0 to 174 kPa. The human physiological temperature of 37 °C changed the overall sensitivity of the sensor. Fig. 2.15 showed the initial capacitances are smaller due to the decrease in relative permittivity of PDMS at higher temperatures [9]. The decrease in relative permittivity of PDMS also decreased the effective permittivity given the Equation 2.4. As the external pressure passed the 75 kPa applied pressure, the test performed at 37 °C showed a higher slope which translated to a higher sensitivity of S = 0.023 kPa^{-1}. A change in temperature and presence of humidity caused a temperature drift. The

effective permittivity change was caused by the instability of environmental conditions as the relative permittivity of air also changed with the temperature [29]. This project used a thermometer to maintain the temperature but it might be that there were some fluctuations unobserved during the long exposure of heat. Even the small sensitivities of the permittivity of air to temperature were enough to observe the shift. The effects due to the permittivity of air diminished as the compression continued decreasing the volume of air pockets. Weadon et al. showed that capacitance changes were higher at increased temperatures when their filler fractional volume decreased as the pressure was applied [28]. The increase from 19 °C to 37 °C resulted in a 28% increase in sensitivity and a 26.6% difference in sensitivities with an error of S = 0.235 kPa^{-1}. The results show that the sensor can be used at a fixed temperature in a controlled environment to eliminate the shift.

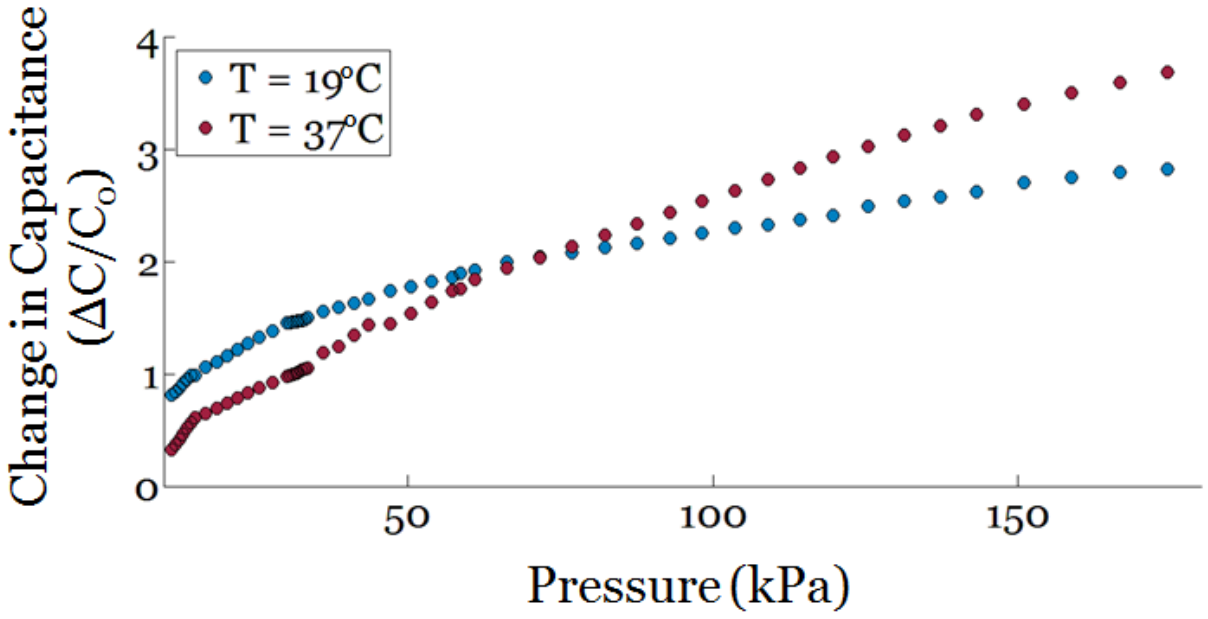

Figure 2.15: Capacitance change (measured at 1 MHz) for the 19:1 PDMS ratio at temperatures 19 °C and 37 °C. The legend indicates the environmental temperature for the experiment. The test performed at 37 °C has an overall greater change but the slope looks similar to its

performance at 19 °C. The slope of the red data points, corresponding to the warmer temperature of 37 °C, started with less of a change in capacitance due to the changes in dielectric properties at other temperatures. The results for the pressure tests at 37 °C showed promising sensitivity and for the dielectric with a 19:1 PDMS base agent to curing agent ratio. Sensor A performed with a sensitivity of S= 0.023 kPa^{-1}. Additional temperature test are required to get a better understanding of the temperature dependence from the dielectric properties.

2.6 Analysis

The 19:1 PDMS ratio, sensor A, appeared to have the highest sensitivity of S = 0.0173 kPa^{-1} when tested at a pressure range from 0 to 174 kPa at a room temperature of 19 °C. After performing the second part of the experiment, sensor A performed with an even higher sensitivity of S = 0.023 kPa^{-1} when tested at a temperature of 37 °C. For this reason, the results were compared to other work. The pressure ranges were selected to match that of previous work done and then the sensitivities were calculated (Table 2.2). The sensor was also compared to the resistive pressure sensor (Table 2.3).

Table 2.2: Sensitivities of 19:1 PDMS ratio at 37°C compared to other research.

This work	Author	Pressure Ranges	Sensitivity reported by Author	Microporous dielectric used by Author
S= 0.023 kPa^{-1}	Chen et al. [5]	0.33 to 250 kPa	S=0.01 kPa^{-1}	Yes
S=0.031 kPa^{-1}	Kwon et al. [4]	30 to 130 kPa	S=0.077 kPa^{-1}	Yes
S=0.29 pF/N	Dinh et al. [6]	0 to 6 N	S=0.012 pF/N	No
S=0.29 pF/N	Molla et al. [7]	0.45 to 1 N	S= 0.06 pF/N	No

Table 2.3: Sensitivities of the 19:1 PDMS ratio capacitive sensor compared to the commercial resistive sensor.

This work	Resistive sensor	Pressure Ranges
S = 0.0626 kPa^{-1}	S = 0.0595 kPa^{-1}	0 to 15 kPa

The pressure sensors with the solid dielectrics did not compare in sensitivity with the performance of the microporous dielectric in this work. The micropores were one advantage for sensitivity. This work also showed a greater sensitivity than the work done by Chen et al from the addition of micropores with the varying PDMS mixing ratios [5]. The work done from Kwon et al. showed a greater sensitivity that might have resulted from fabricating a larger sensor with an area of 12 mm x 12 mm.

Analysis of pressure sensors and their performances found in published articles compared their findings in terms of responsiveness. An important characteristic missing from other works is the true sensitivity of the device given the noise present in their devices to give a complete description of the sensor's sensitivity. The noise can come from parasitic capacitance or measuring devices [30]. This work focuses on the noise caused by the transduction process. The noise spectral density (i.e. sensitivity per square root hertz) was calculated by determining the changes of responsiveness in rms pressure of the device over the bandwidth [31]. The standard deviation in over a fixed pressure of 174 kPa was plotted over the square root hertz (Figure 2.16). The noise spectral density, given by the slope of the graph, was 8.617 $mPa/\sqrt{\text{Hz}}$. The sensitivity in mPa decreased as the frequency increased. This method was used to establish a reliable estimate of the resolution of the sensor.

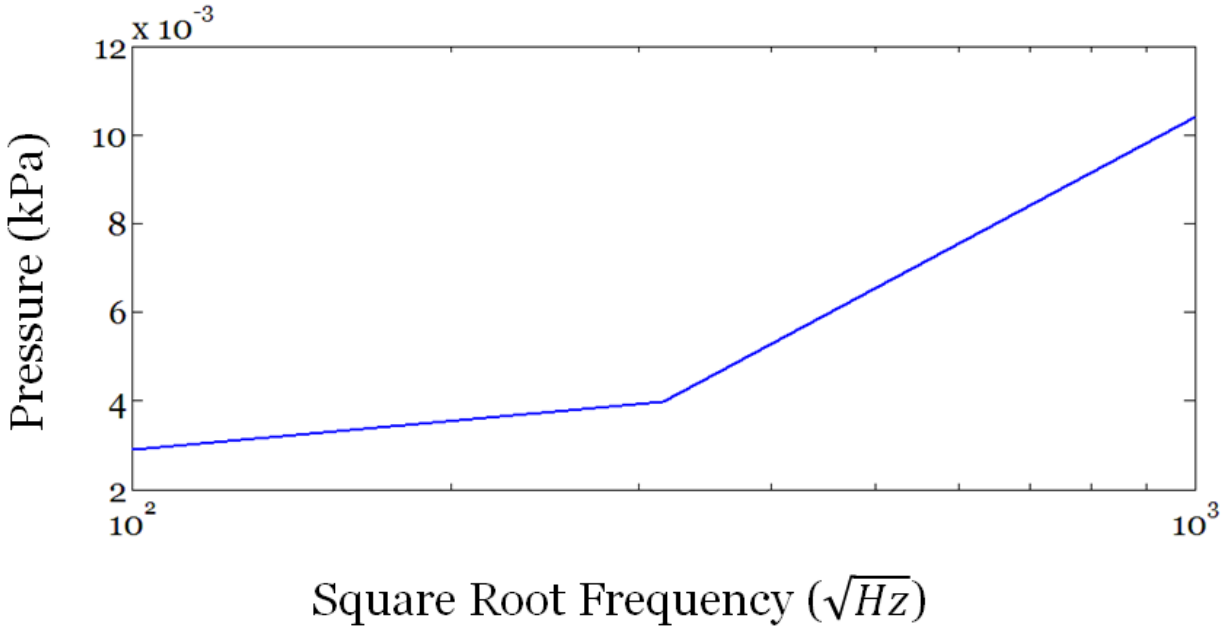

Figure 2.16: The responsivity of the device in kPa over the frequency in square root hertz. The wider bandwidth corresponds to an increase in transduction noise.

Overall, the sensor showed promising sensitivities and responsiveness of changes in capacitances to the changes of pressure compared to other devices. A reliable sensitivity test should be performed on all work reported by calculating the spectral noise density. Thermal noise is another factor that could be limited with additional test done at different temperatures before the continuation of testing under surgical environmental conditions.

Chapter 3

Conclusions and Future Work

3.1 Conclusions

The cost-effective and straightforward fabrication process resulted in five different microporous capacitive sensors. The performance of the microporous capacitors has demonstrated different values in sensitivity with the changes in PDMS ratios and addition of granulated sugar when tested at a pressure range from 0 to 174 kPa. The sensors were fabricated to achieve a low profile of 3 mm x 3 mm x 1 mm. The sensor with 19:1 PDMS mixing ratio showed reproducible properties. The results of sensitivity for the 19:1 PDMS ratio at 19 °C and 37 °C were S= 0.0173 kPa^{-1} and S = 0.023 kPa^{-1}, respectively. The results showed that additional tests should be performed in various temperatures to determine the effects of thermal noise and changes in capacitance. The effective permittivity changes were calculated as well as the spectral noise density to characterize the sensitivity of the device. The effective permittivity was calculated to be $\varepsilon_{effective}$ = 1.825 ± 0.051 and a porosity of 50% from the air pockets. The noise spectral density was 8.617 $mPa/\sqrt{Hz}$ which established a reliable estimate of the resolution of the sensor.

The sensor showed a dynamic response time of 0.29 ± 0.17 seconds and an average pore size of 289 ± 135 μm. The dynamic response time of the sensor aided by the micropores and

elastic properties from the change in curing agent show reliable applications of this sensor in the medical industry. The fast response of the sensor will be able to give the surgeon accurate feedback and be used to fulfill the physician's task of implementing a sensor in surgical tools during surgery. The device could also be applied for non-invasive purposes. The sensor is also ready for waterproofing to be tested under fluidic conditions. Future work involves mounting the sensor on the surgical instruments and tested under the supervision of a physician. With the dimensions and performance results from these tests, the 19:1 PDMS ratio sensor is ready for real-time analysis under similar surgical environments. This work shows progress in microporous capacitive pressure sensors with varying PDMS base agent to curing agent ratios.

3.2 Future of Sensors in Healthcare

Sensors in healthcare are customizable depending on the environment for invasive and non-invasive monitoring. A dependable device is challenging to fabricate for this reason. Many fabrication methods have been tested to achieve the highest sensitivity. This project shows promises for use in variable monitoring i.e. surgical pressure sensing and self-monitoring. Future work for a surgical sensor involves mounting the sensor onto a cystoscope. The cystoscope will be placed in a wet and warm environment. The electromechanical performance will be shown processed and shown in real time for the surgeon to easily follow. The processed data will also need to be archived for long periods of time so that he may go back and analyze the data at a later time post-surgery.

In parallel, the sensors can be made to be wider or made into an array to use as a self-monitoring sensor. The sensor will be made into a patch that the patient can place anywhere outside of the body. The high sensitivity shows promise in dependability. Of course, this sensitivity can be improved by further improving the fabrication process. The granulated

sucrose was mixed with the PDMS but there are several types of sugar e.g. molasses, raw, and powdered. The pores sizes will differ from sugar type and can change the elastomer properties.

Another change to the sensor is the electrode type. Copper was chosen because it was thin and inexpensive, however, it is very reactive and not used inside the body unless it is completely sealed. The additional sealant to copper would require more work and might increase the thickness of the sensor. The sealant might prove to be advantageous because of its waterproofing capabilities.

Bibliography

[1] Konstantinova, A. Jiang, K. Althoefer, P. Dasgupta and T. Nanayakkara, "Implementation of Tactile Sensing for Palpation in Robot-Assisted Minimally Invasive Surgery: A Review", *IEEE Sensors Journal*, vol. 14, no. 8, pp. 2490-2501, 2014.

[2] P. Puangmali, K. Althoefer, L. Seneviratne, D. Murphy and P. Dasgupta, "State-of-the-Art in Force and Tactile Sensing for Minimally Invasive Surgery", *IEEE Sensors Journal*, vol. 8, no. 4, pp. 371-381, 2008.

[3] S. Kang, J. Lee, S. Lee, S. Kim, J. Kim, H. Algadi, S. Al-Sayari, D. Kim, D. Kim and T. Lee, "Highly Sensitive Pressure Sensor Based on Bioinspired Porous Structure for Real-Time Tactile Sensing", *Advanced Electronic Materials*, vol. 2, no. 12, p. 1600356, 2016.

[4] D. Kwon, et al., "Highly Sensitive, Flexible, and Wearable Pressure Sensor Based on a Giant Piezocapacitive Effect of Three-Dimensional Microporous Elastomeric Dielectric Layer", *ACS Applied Materials & Interfaces*, vol. 8, no. 26, pp. 16922-16931, 2016.

[5] S. Chen, B. Zhuo and X. Guo, "Large Area One-Step Facile Processing of Microstructured Elastomeric Dielectric Film for High Sensitivity and Durable Sensing over Wide Pressure Range", *ACS Applied Materials & Interfaces,* vol. 8, no. 31, pp. 20364-20370, 2016.

[6] T. Dinh, E. Martincic, E. Dufour-Gergam and P. Joubert, "Experimental study of PDMS mechanical properties for the optimization of polymer based flexible pressure micro-sensors", *Journal of Physics: Conference Series*, vol. 757, p. 012009, 2016.

[7] S. El-Molla, et al., "Integration of a Thin Film PDMS-Based Capacitive Sensor for Tactile Sensing in an Electronic Skin", *Journal of Sensors*, vol. 2016, pp. 1-7, 2016.

[8] K. Lei, K. Lee and M. Lee, "Development of a flexible PDMS capacitive pressure sensor for plantar pressure measurement", *Microelectronic Engineering*, vol. 99, pp. 1-5, 2012.

[9] C. Pang, J. Koo, A. Nguyen, J. Caves, M. Kim, A. Chortos, K. Kim, P. Wang, J. Tok and Z. Bao, "Highly Skin-Conformal Microhairy Sensor for Pulse Signal Amplification ", *Advanced Materials*, vol. 27, no. 4, pp. 643-640, 2015.

[10] W. Gao, S. Emaminejad, H. Nyein, S. Challa, K. Chen, A. Peck, H. Fahad, H. Ota, H. Shiraki, D. Kiriya, D. Lien, G. Brooks, R. Davis and A. Javey, "Fully integrated wearable sensor arrays for multiplexed in situ perspiration analysis", *Nature*, vol. 529, no. 7587, pp. 509-514, 2016.

[11] B. Tee, A. Chortos, R. Dunn, G. Schwartz, E. Eason and Z. Bao, "Tunable Flexible Pressure Sensors using Microstructured Elastomer Geometries for Intuitive Electronics", *Advanced Functional Materials*, vol. 24, no. 34, pp. 5427-5434, 2014.

[12] M. Hessinger, T. Pilic, R. Werthschutzky and P. Pott, "Miniaturized force/torque sensor for in vivo measurements of tissue characteristics", *2016 38th Annual International Conference of the IEEE Engineering in Medicine and Biology Society (EMBC)*, 2016.

[13] "Tekscan | Pressure Mapping, Force Measurement, & Tactile Sensors", Tekscan, 2016. [Online]. Available: https://www.tekscan.com/. [Accessed: 10- Dec- 2016].

[14] P. Saccomandi, E. Schena, C. Oddo, L. Zollo, S. Silvestri and E. Guglielmelli, "Microfabricated Tactile Sensors for Biomedical Applications: A Review", *Biosensors*, vol. 4, no. 4, pp. 422-448, 2014.

[15] T. Grove, M. Masters and R. Miers, "Determining dielectric constants using a parallel plate capacitor", *American Journal of Physics*, vol. 73, no. 1, pp. 52-56, 2005.

[16] G. Carlson and B. Illman, "The circular disk parallel plate capacitor", *American Journal of Physics*, vol. 62, no. 12, pp. 1099-1105, 1994.

[17] B. Wells, E. Baker, A. Farwell, H. Foster, X. Gao, B. Gruber, E. Jones, D. Vu, S. Xu and J. Ye, "An adjustable parallel-plate capacitor instrument—Test of the theoretical capacitance formula", *American Journal of Physics*, vol. 84, no. 9, pp. 723-726, 2016.

[18] M. Albouelwafa and E. Kendall, "Analysis and design of helical capacitance sensors for volume fraction determination", *Review of Scientific Instruments*, vol. 50, no. 7, pp. 872-878, 1979.

[19] O. Schneegans, P. Chrétien, F. Houzé and R. Meyer, "Capacitance measurements on small parallel plate capacitors using nanoscale impedance microscopy", *Applied Physics Letters*, vol. 90, no. 4, p. 043116, 2007.

[20] T. Ishii, M. Endo, K. Masuda and K. Ishida, "The possibility of giant dielectric materials for multilayer ceramic capacitors", *Applied Physics Letters*, vol. 102, no. 6, p. 062901, 2013.

[21] H. Vandeparre, D. Watson and S. Lacour, "Extremely robust and conformable capacitive pressure sensors based on flexible polyurethane foams and stretchable metallization", *Applied Physics Letters*, vol. 103, no. 20, p. 204103, 2013.

[22] L. Hadfield-Law, "Male catheterization", *Accident and Emergency Nursing*, vol. 9, no. 4, pp. 257-263, 2001.

[23] M. Kalantari, M. Ramezanifard, R. Ahmadi, J. Dargahi and J. Kövecses, "A piezoresistive tactile sensor for tissue characterization during catheter-based cardiac surgery", *The International Journal of Medical Robotics and Computer Assisted Surgery*, vol. 7, no. 4, pp. 431-440, 2011.

[24] A. Kuo, *"Poly (dimethylsiloxane)." Polymer data handbook*, 1st ed. Oxford University Press, Inc., 1999, pp. 411-435.

[25] N. Pennington and C. Baker, *Sugar*, 1st ed. New York: Van Nostrand Reinhold, 1990, pp. 48-61, 280-285.

[26] M. Asadi, *Beet-sugar handbook*, 1st ed. Hoboken (N.J.): Wiley-interscience, 2007, pp. 473-478.

[27] "SYLGARD® 184 SILICONE ELASTOMER KIT", *Dowcorning.com*, 2017. [Online]. Available: http://www.dowcorning.com/applications/search/default.aspx?R=131EN. [Accessed: 11- Apr- 2017].

[28] T. Weadon, T. Evans and E. Sabolsky, "An Analytical Model for Porous Polymer-Ceramic Capacitive Pressure Sensors", *IEEE Sensors Journal*, vol. 14, no. 12, pp. 4411-4422, 2014.

[29] A. Heidary, "A Low-Cost Universal Integrated Interface for Capacitive Sensors", Master of Science, Tehran University, Tehran, Iran, 2010.

[30] Whitaker, *The electronics handbook*, 1st ed. Boca Raton, FL: CRC Press, 2005, pp. 620-680.

[31] R. Spender, B. Fleischer, P. Barth and J. Angell, "A theoretical study of transducer noise in piezoresistive and capacitive silicon pressure sensors", *IEEE Transactions on Electron Devices*, vol. 35, no. 8, pp. 1289-1298, 1988.